Numerical Study of Stirring Effects in a Mode-Stirred Reverberation Chamber by using the Finite Difference Time Domain Simulation

Jong-Sung Kim[(1)] and Raj Mittra[(2)]

[(1)] Dept. of Information and Communications Eng., Kyungsung Univ., Korea

(Email: jskim@ks.ac.kr)

[(2)] Dept. of Electrical Eng., Pennsylvania State Univ., PA, USA

(Email: mittra@engr.psu.edu)

Abstract— The spectral field data on the observation planes inside a mode-stirred chamber, which describe the directional dependence of all supported modes in the reverberation chamber, are computed by using the FDTD method. Correlation coefficients are computed to evaluate the efficiency of the mode stirrer for three different sizes of stirrers. The spectral characteristics of the stirring effects in a reverberation chamber are investigated by using the conventional statistical analysis to determine the uniformity of the spatial electric fields.

Index Terms— Spectral analysis, correlation coefficient, reverberation chamber, statistical analysis.

I. INTRODUCTION

A reverberation chamber (RC) typically consists of a metallic cavity and a rotating metallic stirrer, which enables us to change the field behavior inside the cavity. Spatial field distribution inside the RC is perturbed by the rotating stirrer in order to produce a field behavior which is close to being statistically uniform and isotropic, implying nearly equal power is incident from all directions with all polarization components, when averaged over a number of stirrer positions. The stirrer, usually in the form of several metallic paddles, helps to generate a statistically uniform environment within the chamber. Although a wide variety of different types of mode stirrers have been used in the past, there has been little research carried out to evaluate the performance of these mode stirrers. It has been stated in [1] that stirrers should have dimensions that are a significant fraction of the chamber dimensions and of the wavelength at the lowest usable frequency. However, no detailed guidelines have been provided in the above work for building highly efficient stirrers. In addition, although not obvious, it has been found that a relatively small and simple stirrer inside a highly complex cavity can produce a field which is statistically more uniform than that generated by a large complex stirrer placed inside a simple cavity with smooth wall surfaces.

In [2], J. Clegg has investigated stirring effects produced by four different designs by using a genetic algorithm in order to optimize the design of the stirrer. However, the author has employed an optimization-based design, which provides little intuition, or clues as to the limitations in practical applications.

In [3], Arnaut has quantified the performance of an RC by the number of coherence cells traversed during the stirring process and the number of mode-count. However, this approach is unable to handle fine geometries of mode stirrers. The work by Wellander[4] has described the stirring effect only by the lowest usable frequency, but it did not utilize the statistical uniformity criterion as a measure of efficiency of the stirrer.

In this paper, we review the spectral evaluation process of the stirring effects in a reverberation chamber by using the Finite Difference Ttime Domain (FDTD) method [5]-[6], and then compare with the results with those derived from the conventional statistical analysis to determine the uniformity of the spatial electric fields. We utilize the fact that the field uniformity and isotropy inside the working volume of the RC can be estimated by computing the spectral fields and correlation coefficients for an entire range of stirring angles.
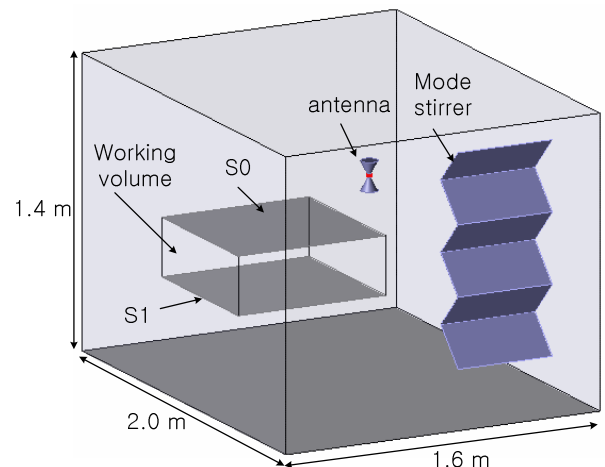

Fig. 1. Geometry of the reverberation chamber with a biconical antenna, a mode stirrer, a working volume, and two observation planes.
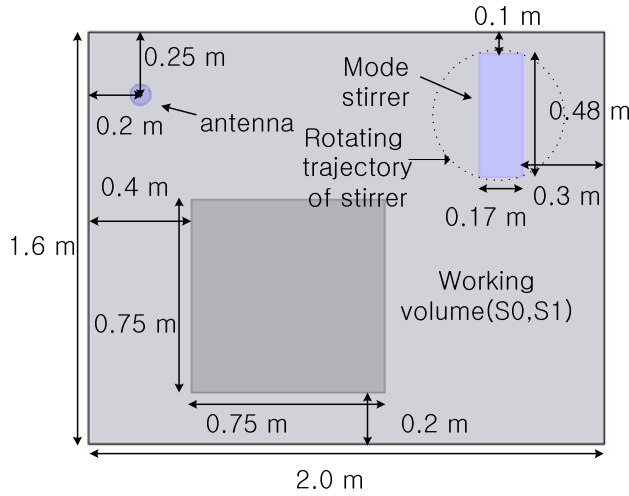
Fig. 2. Cross section of the reverberation chamber. Dimensional data of two observation planes and a mode stirrer with its rotation area are shown.

II. SPECTRAL CONTENTS OF OBSERVED ELECTRIC FIELDS

The geometry of the RC investigated is depicted in Fig. 1. The dimensions of the RC are 2.0 (W) x 1.6(L) x 1.4 (H) m^3, and a vertically oriented and z-folded mechanical stirrer is inserted within this chamber. The fundamental resonant frequency of the RC is approximately 120 MHz, and the lowest usable frequency (LUF) is about 500 MHz. The cross-sectional view of the exciting antenna, mode stirrer, and the working volume are depicted in Fig. 2, in which the sizes and positions of all the elements are designated. The RC is excited by using a vertically-oriented bi-conical antenna with a cone angle of 50°, and a length of 120 mm. The mode stirrer has the dimensions of 0.17 (W) x 0.48 (L) x 1.02 (H) m^3, and it rotates around its center point. The excitation antenna and the mode stirrer are located at the mid-points along the

vertical direction of the RC. The electric fields have been observed on two planes, namely, the upper and lower surfaces of the working volume, S0 and S1, in order to evaluate the stirring effects. The dimension of the working volume is 0.75 (W) x 0.75 (L) x 0.28 (H) m^3 at the height of 0.3 m from the bottom of the chamber. In general, it is desirable to investigate the low frequency limit of the RC, which determines the range of its usefulness for practical applications.

The RC was simulated for the frequency band ranging from 500 MHz to 5.0 GHz. The stirrer geometry was divided into a grid of 399 x 320 x 274 cubic cells, and a non-uniform meshing with a minimum cell size of 5.0 mm was used. The vertical six-paddle stirrer was incrementally rotated, using an angular step of 15°, between the range of 0° and 345°. The effect of the rotating stirrer can be observed by the changes in the field values on S0 and S1 of Fig. 1, where the large E-field variations over one revolution of the stirrer verify its effectiveness, even for relatively low frequencies. The orthogonal electric field components on two observation planes, namely S0 and S1, are stored at 46 frequency points, with a frequency step of 100 MHz within the band of interest. The S0 and S1 planes are divided into 150x150 cells, along the x and y directions. Fig. 3 shows the spectral distributions of Ez field obtained at 0.5 GHz on S0, for stirrer angles of 0°, 15°, and 45° derived by converting the observation data found in the FDTD calculation via Fourier transformation. The magnitudes of the E_z-component indicated by the color bar are displayed by the normalized wave numbers to k0, along the x- and y-directions, respectively. A unit circle is included as a boundary indicator of mode propagation in the chamber. The directional dependence of the wave propagation at each angle can be seen from Fig. 3. The perturbation effect introduced by the rotating stirrer can be clearly observed from the spectral distribution behavior of the plot. The spectral variations of E_z
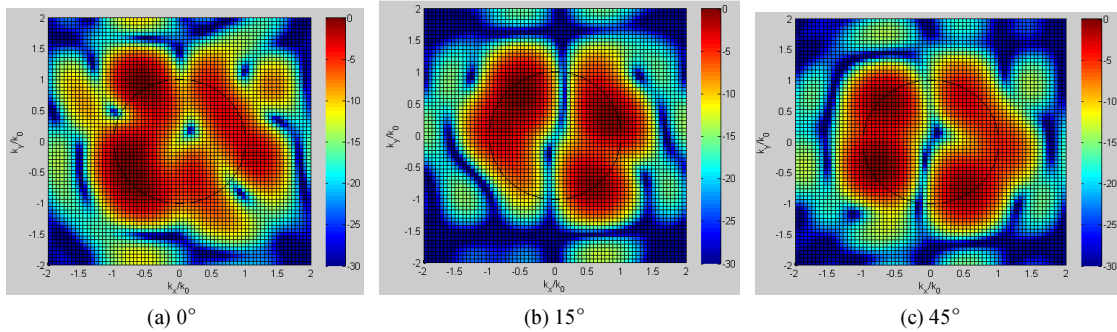

(a) 0° (b) 15° (c) 45°

Fig. 3. Spectral distribution of E_z field component on the S0 plane over a rotating mode stirrer at 0.5 GHz

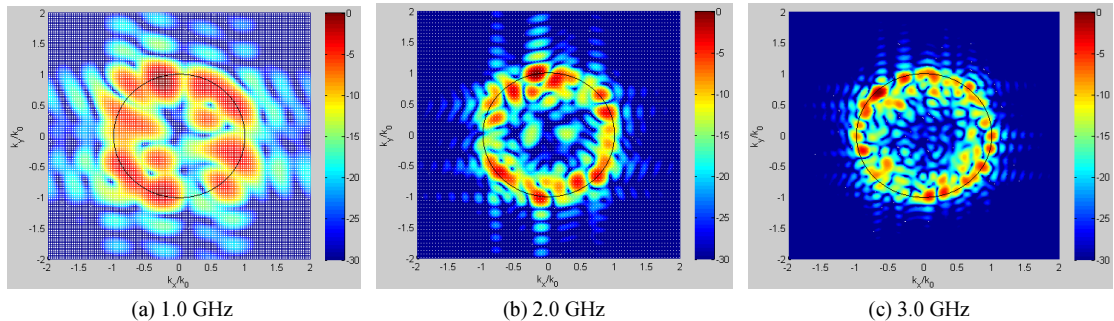(a) 1.0 GHz (b) 2.0 GHz (c) 3.0 GHz

Fig. 4. Spectral distribution of E_z field component on the S1 plane at 1.0, 2.0, and 3.0 GHz

2

field at 1.0, 2.0, and 3.0 GHz on S1 are displayed in Fig. 4. We note that the number of propagation modes increases as we increase the observation frequencies. Frequency region near the origins of Fig. 3 and 4 indicates non-propagation at low frequencies that fall below the fundamental resonant frequency of the RC. The asymmetries of all the spectral distributions are attributed to the existence of the stirrer and the excitation source inside the RC.

III.   COMPARISON OF THREE TYPES OF MODE STIRRERS

The mode stirrers considered in this paper consist of six PEC paddles, with a connection angle of 90°, as shown in Fig. 5. Three different designs of the mode stirrer are considered. Their vertical shapes are chosen to be the same for the sake of consistency, though their horizontal geometries are different. The mode-stirrers appearing in Figs. 1 and 2 are identical to the stirrer-1 in Fig. 5(a). Stirrer-2 and stirrer-3 are implemented by reversing and removing the right-half section of the stirrer-1 in Fig. 5(a). Stirrer-3 has one half the cross-section of either stirrer 1 or 2, but its rotational cross section is the same as those of the others, as specified by the axis of rotation (AOR) in Fig. 5. Stirrer-1 is 1.018 m high with diameter of 0.48 m. The heights (1.018 m) of stirrer-2 and -3 are the same size as that of stirrer-1, but they have different lengths. The length of the stirrer-3 is half the length of stirrer-2 or -3, but its swept volumes of all three stirrers are the same. The moving area inside the RC is shown in Fig. 2.

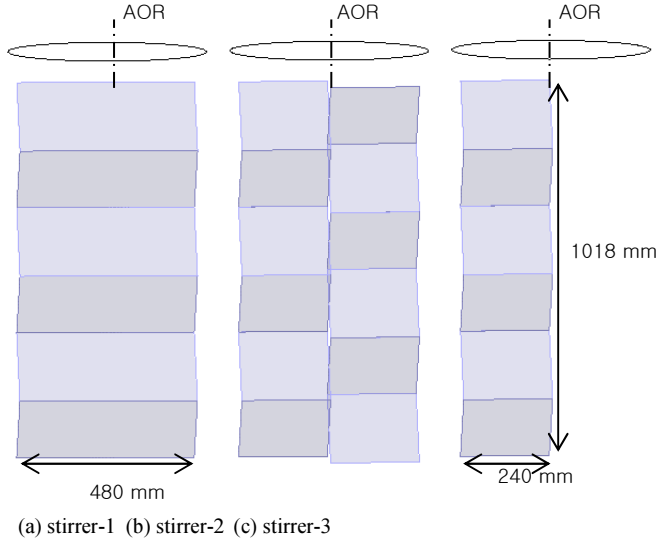(a) stirrer-1 (b) stirrer-2 (c) stirrer-3

Fig. 5. The geometry of stirrers simulated

Next, we compute the correlation coefficient in order to investigate the independence of the field distributions as the function of the stirrer rotation. The correlation coefficient of zero represents the desired goal, and this correlation coefficient is evaluated by using:

$$\rho = \frac{\sum_m \sum_n (E_{mn}^{\theta_1} - \overline{E}^{\theta_1})(E_{mn}^{\theta_2} - \overline{E}^{\theta_2})}{\sqrt{(\sum_m \sum_n (E_{mn}^{\theta_1} - \overline{E}^{\theta_1})^2)(\sum_m \sum_n (E_{mn}^{\theta_2} - \overline{E}^{\theta_2})^2)}}$$

where E^{θ_1} and E^{θ_2} represent the two sets of the spectral electric fields to be compared, and $\overline{E}^{\theta_1}$ and $\overline{E}^{\theta_2}$ are their corresponding mean values. The spectral electric fields were found at 24 stirrer angles from 0° to 345°. The correlation coefficients have been calculated between all possible combinations of two different angles of a rotating stirrer. Fig. 6 shows all the combinations of the correlation coefficients between spectral electric fields on S0 for 24 rotation states of stirrer-1 within the RC, at the frequencies of 0.5, 1.0, and 3.0 GHz. The observed field on the S1 plane of Fig. 1 showed a similar trend. The correlation coefficients of 276 combinations for 24 angle-states of stirrer-1 have been computed. It is found that the independence at a higher frequency, i.e., low correlation coefficient, is stronger than it is at a lower frequency, as has been predicted by previous publications on this topic.

Fig. 7 shows the mean value and standard deviation of correlation coefficients in the frequency band of 0.5-5.0 GHz for three types of stirrers. It is observed that there are clear differences in the characteristics of the three stirrers. The mean values and standard deviations of the correlation coefficients at the lower frequencies are all higher, and this can be attributed to the small number of excitation modes at the region and small changes of field distributions by a rotating stirrer. At higher frequencies, there are large changes in the field distributions as the stirrer is rotated, due to an increase in the number of guided modes. The independence of the stirrer-1 is the strongest among the three, i.e., those of the stirrer-2 and -3 are relatively inferior. While the mean values of stirrer-2 are lower than those of stirrer-3, we note that the standard deviations of stirrer-2 are larger than those of stirrer-3 for all the frequencies of observation. This is attributable to the fact that stirrer-2 has a more symmetric rotational shape, which has been realized by reversing the right and left sections of the same.
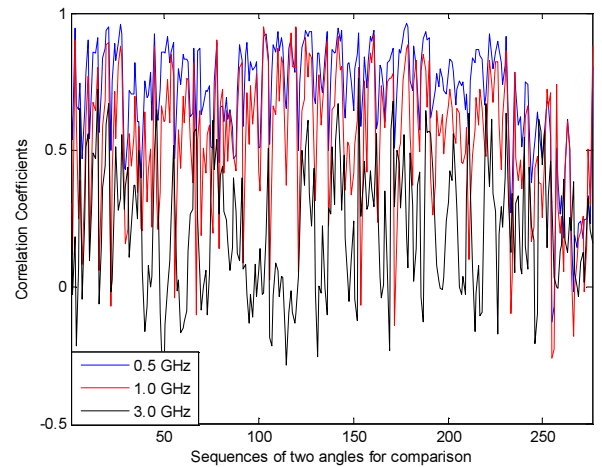

Fig. 6. All correlation coefficients for 24 moving angles of a rotating stirrer

It is found that higher the excitation frequency, more uniform is the field in the RC. The low correlation coefficients at higher frequency indicate that stirring effects are more

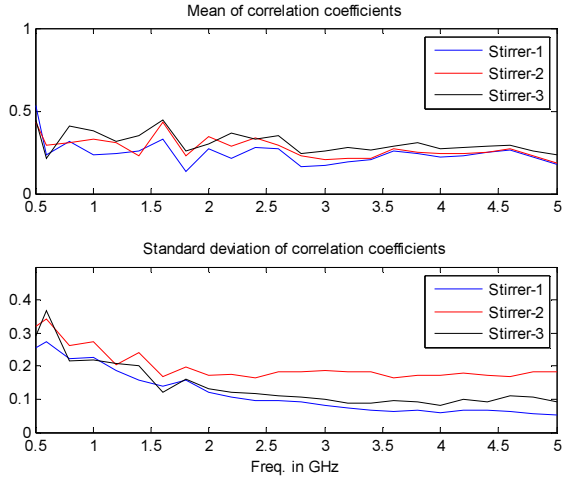effective at these frequencies than they are at the lower frequencies.

Fig. 7. Mean and standard deviation values of all combinations of correlation coefficients for the spectral fields in the observation planes for 24 rotation angles of three stirrers in the frequency range of 0.5-5.0 GHz.

IV. COMPARISON WITH STATISTICAL RESULTS

Intuitively, a good stirrer might be expected to modify the fields significantly from that of an empty RC. However, it is not clear whether the change should be in magnitude, in direction, or both. One way to asses the effectiveness of various stirrers is to compare their performances of various stirrers to determine which stirrer-shape performs better than the others. The moving areas of the stirrers are kept as similar as possible so that comparisons are made on the basis of the shape of the stirrer, rather than its size.

We have investigated the electric field values resulting from the FDTD simulations as the stirrer is rotated. The three components E_x, E_y, and E_z are evaluated at the two surfaces in the working volume, for each position of the stirrer, in order to evaluate the stirring effect on the spectral fields. Spatial electric fields are determined at frequencies ranging from 0.5-5.0 GHz. The standard deviation of the total electric field, as shown in Fig. 8, is derived by storing all the electric fields in x-, y-, and z-directions at the two observation planes of 150x150 cell dimensions for each stirrer position. Though there are large field variations at lower frequencies, uniformity is achieved at frequencies above 1 GHz [7]-[8].

The stirrer-2 is not expected to perform as well as the others since its moving shape is more symmetrical, compared to that of stirrer-3, which has half the size of stirrer-2. It has been reported in [9] that increasing the size and asymmetry of the stirrer will improve its performance, and the present study verifies the above claim. It is possible to determine the sizes of the working volumes by using the 3 dB criterion for the standard deviation for the lowest usable frequencies for the three types of stirrers investigated.

V. CONCLUSIONS

The spectral field contents on two surfaces of the working volume inside an RC have been computed and used to investigate the stirring effects. It is possible to estimate the perturbation effects of the rotating mode stirrer by finding all the correlation coefficients between spectral electric fields for combinations of two angles of a rotating stirrer. Three types of z-shaped stirrers have been considered. Field uniformity and isotropy inside the working volume of the RC have been verified after computing the spectral fields and correlation coefficients for all the stirring angles. There is a strong relationship between the field uniformity and the correlation coefficients of the fields for the rotating mode stirrers. The approach described in this work is very versatile and relatively independent of the method of, the mechanical, electrical, and platform settings, the design of stirrers and the determination of their locations within the RC.
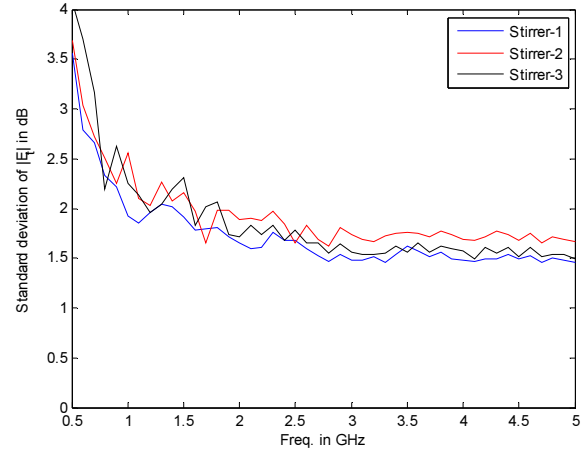

Fig. 8. Standard deviation of total electric fields

REFERENCES

[1] "Electromagnetic Compatibility (EMC) Part 4: Testing and Measurement Techniques Section 21: Reverberation Chamber Test Methods" International Electrotechincal commission, IFC61000-4-21 Draft, 2003.

[2] J. C. Clegg, A. C. Marvin, J. F. Dawson, and S. J. Porter , "Optimization of stirrer designs in a reverberation chamber," *IEEE Trans. Electromagn. Compat.*, Vol. 47, No. 4, pp. 824–832, Nov. 2005.

[3] Luk R. Arnaut, "Effect of size, orientation, and eccentricity of mode stirrers on their performance in reverberation chambers," *IEEE Trans. Electromagn. Compat.*, vol. 48, no. 3, pp. 600-602, Aug. 2006.

[4] N. Wellander, O. Lunden, and M. Backstrom, "Experimental investigation and mathematical modeling of desihn parameters for efficient stirrers in mode-stirrered reverberation chambers," *IEEE Trans. Electromagn. Compat.*, vol. 49, no. 1, pp. 94-103, Feb. 2007.

[5] Jong-Sung Kim, J. Bringuier, and R. Mittra. "Spectral evaluation of stirring effect in a reverberation chamber",

2011 *IEEE International Symposium on Antennas and Propagation (APSURSI)*, pp.3144-3147,July, 2011.

[6] Jong-Sung, Kim and Raj Mittra. "Performance evaluation of a mode-stirred reverberation chamber using the finite difference time domain (FDTD) simulation", *2012 Asia-Pacific Symposium on Electromagnetic Compatibility*, pp.173 – 176, 21-24 May, 2012.

[7] S. Mengue, E. Richalot, and O. Picon, "Comparison between different criteria for evaluating reverberation chamber functioning using a 3-D FDTD algorithm," *IEEE Trans. Electromagn. Compat*., vol. 50, no. 2, pp. 237-245, May 2008.

[8] A. Coates and A. P. Duffy, "Maximum working volume and minimum working frequency tradeoff in a reverberation chamber," *IEEE Trans. Electromagn. Compat*., vol. 49, no. 3, pp. 719-722, Aug. 2007.

[9] D. I. Wu and D. C. Chang, "The effect of an electrically large stirrer in a mode-stirred chamber," *IEEE Trans. Electromagn. Compat*., vol. 31, no. 2, pp. 164–169, May 1989.

Jong-Sung Kim received the BS degree in electronics engineering from Kyungpook National University, Daegu, Korea, in 1988, the MS degree in electrical engineering from Korea Advanced Institute of Science and Technology (KAIST), Seoul, Korea, in 1990, and the Ph.D. degree in electrical engineering from Pohang University of Science and Technology (POSTECH), Pohang, Korea, in 2001. He worked as a member of technical staff at Korea Telecom from 1990 to 2002. He joined the Dept. of Information and Communications Engineering in Kyungsung University in 2004, Pusan, Korea as an assistant professor, where he is now a Professor. His research interests include design and measurement of passive and active microwave circuits and numerical analysis of microwave circuits and antennas.

Numerical Study of Stirring Effects in a Mode-Stirred Reverberation Chamber by using the Finite Difference Time Domain Simulation

Jongsung Kim# and Raj Mittra*

Kyungsung University, Korea
* Pennsylvania State University, PA, USA

Contents

- Geometry of Reverberation Chamber(RC)
- Spectral field distribution in the mode-stirred RC
- Correlation coefficients between any two angles of the rotation mode stirrer in RC
- Comparison of stirring effects for three different stirrers

Geometry of Reverberation Chamber

working volume

S0

mode stirrer

antenna

1.4 m

S1

2 m

1.6 m

3
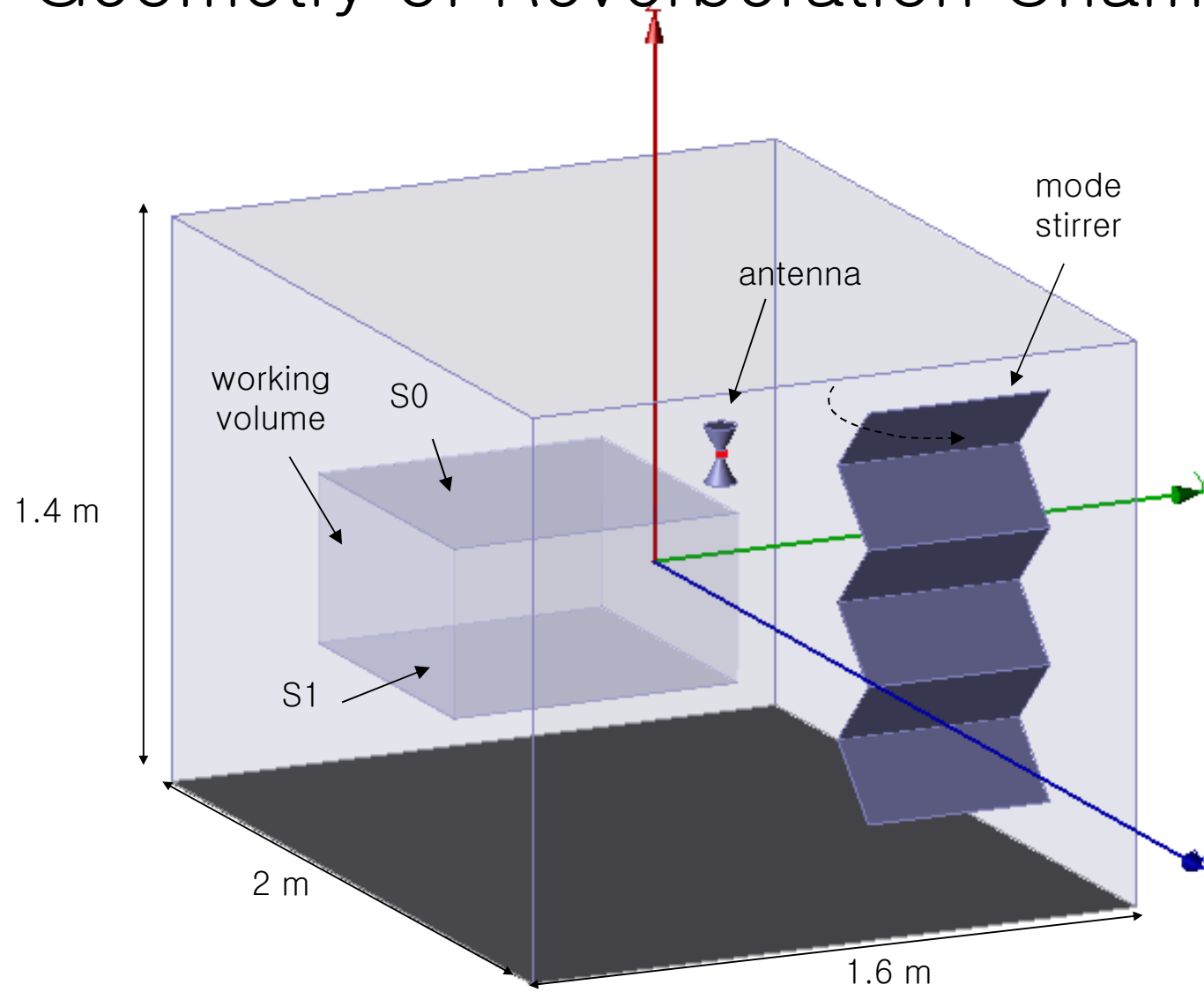
Geometry of Reverberation Chamber (Comments)

This is a typical structure of the RC, which is a metallic cavity surrounded by all metallic walls.

Its dimensions are 2m x 1.6m x 1.4 m.

The exciter antenna is located at the upper right side and a mode stirrer is placed at the upper left side.

This chamber is generally used to provide real field environment inside the metallic type of cavity.

We can measure electromagnetic interference and compatibility of electronic devices or systems in the RC.

For example, we can measure radiation efficiency, diversity gain, or channel capacity of MIMO systems.

The biconical antenna can excite internal fields in the chamber.

The rotating stirrer changes the boundary condition in the cavity.

We generate statistically uniform and isotropic fields by rotating the mode stirrer.

We use two observation planes to observe the field values.

Cross Section of the RC

0.1 m

moving trajectory of stirrer

0.25 m

0.2 m antenna

Mode stirrer

0.48 m

0.3 m

0.17 m

0.4 m

1.6 m

0.75 m

Working volume(S0,S1)

0.75 m

0.2 m

2.0 m

4
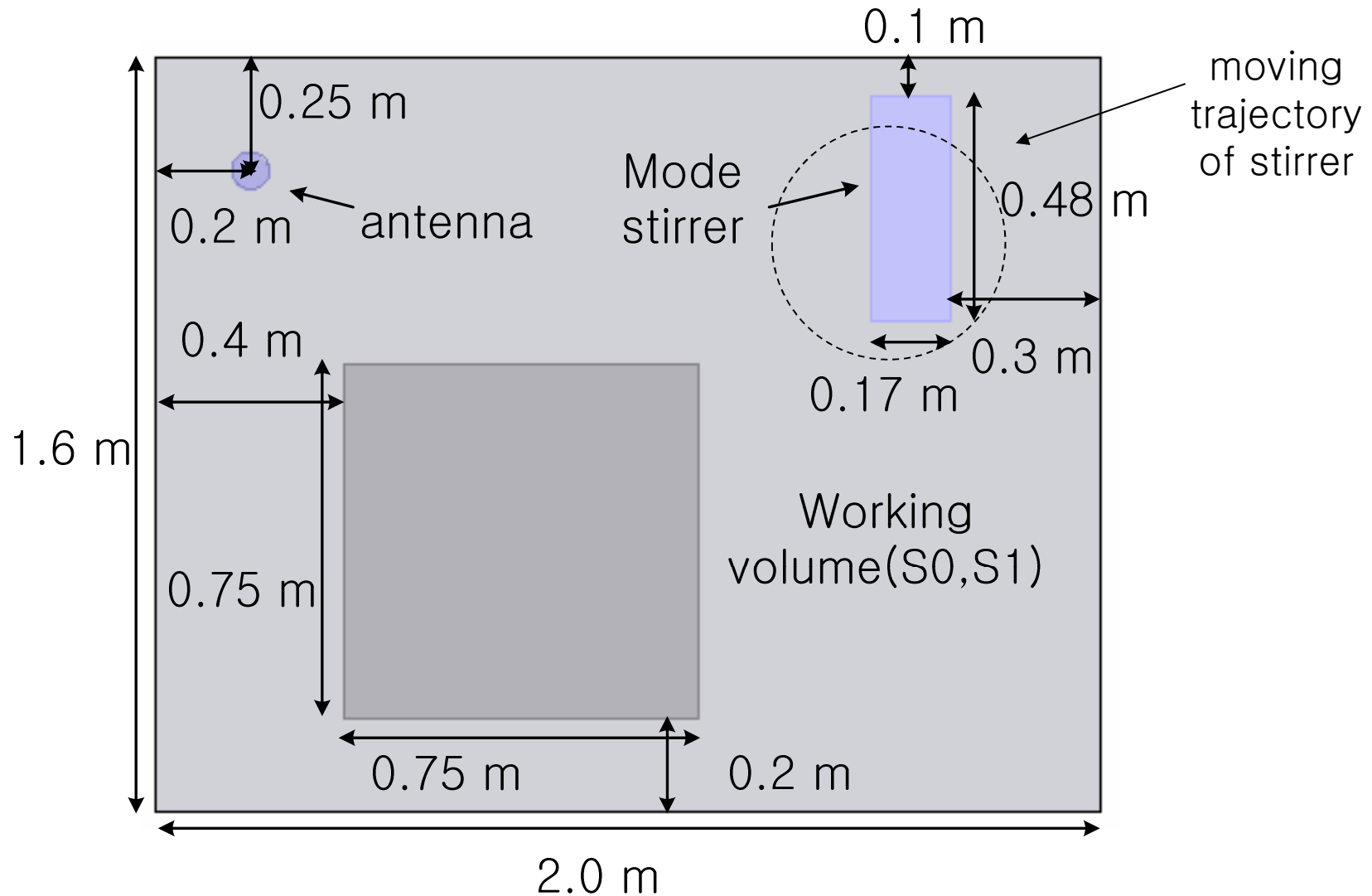
Cross Section of the RC (Comments)

This figure shows the cross-section of our RC.

The excitation antenna is located at the upper left side and the rotating mode stirrer is located at the upper right side.

The circle represents the moving trajectory of the mode stirrer.

On this plane, we will observe the field distributions generated by the source and perturbed by the rotating stirrer.

All geometrical parameters are provided in this figure.

Literature survey
of stirring effects

IEEE T. EMC 2005, J. Andrew et al

Optimization method

IEEE T. EMC 2006, L. Amaut

Number of coherence cells
visited upon rotation
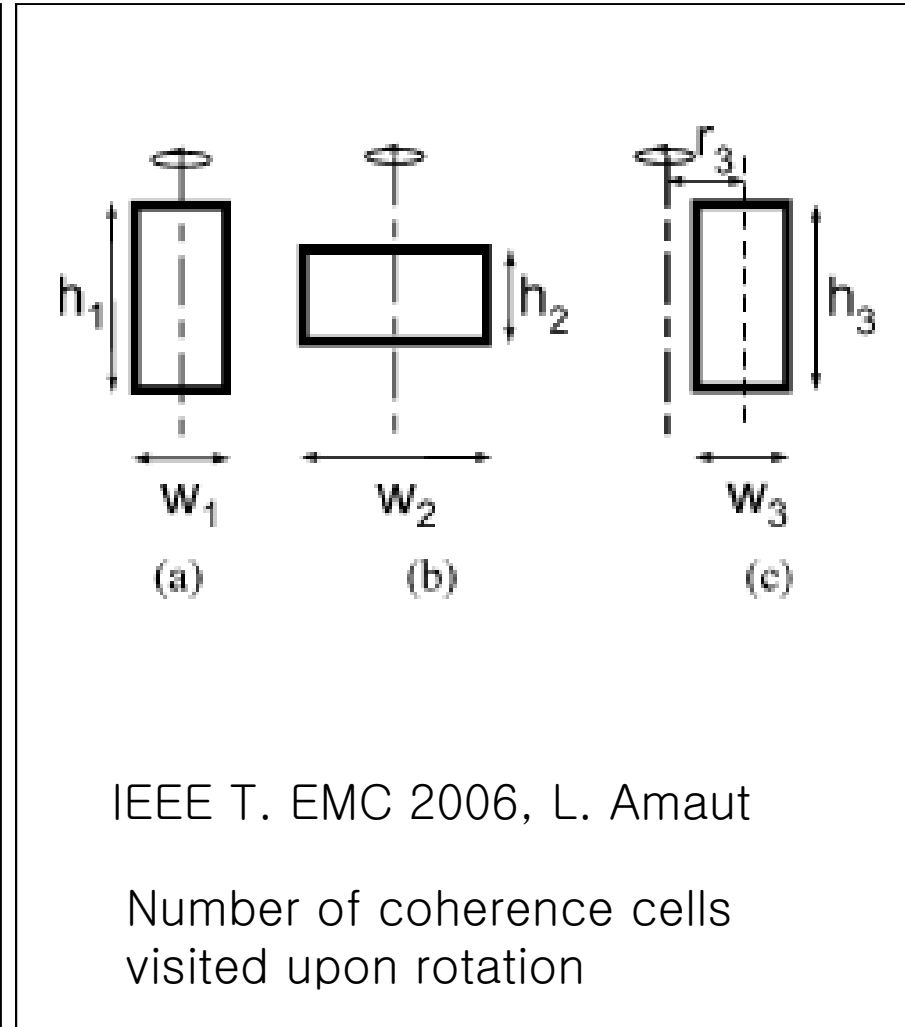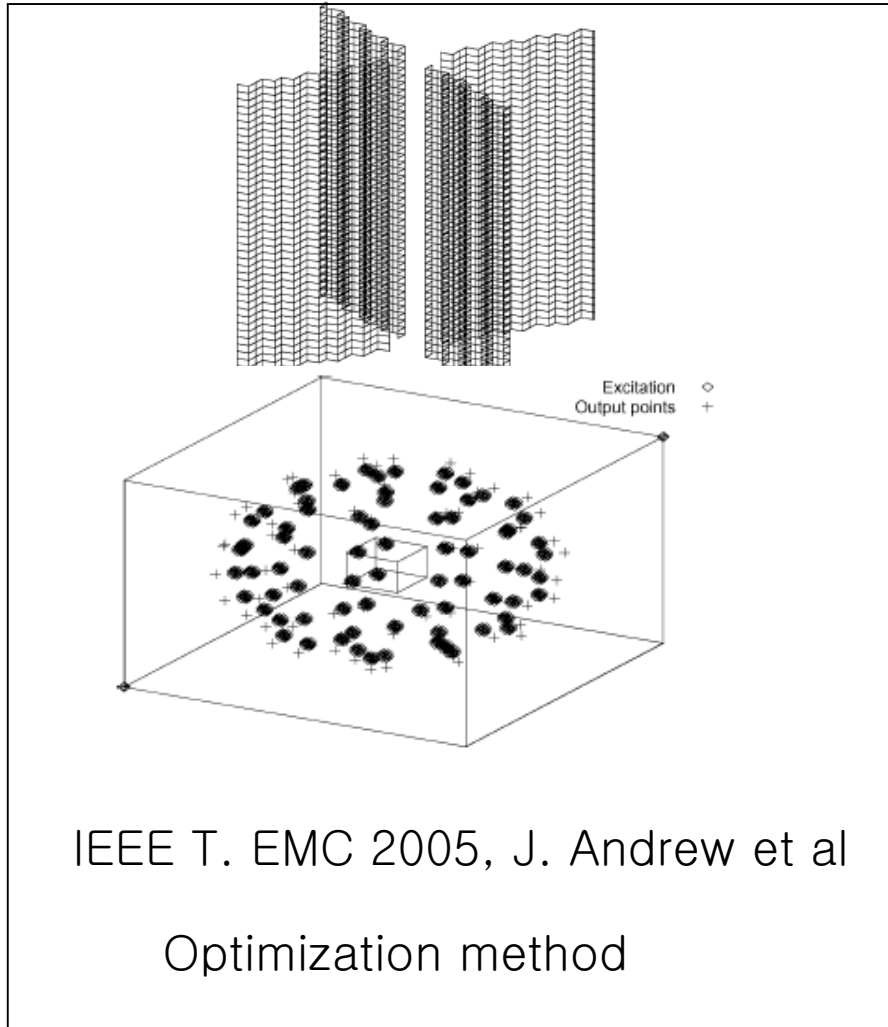
Literature survey of stirring effects (Comments)

The literature surveys related with this talk are shown as follows.

Left one shows the optimization based method proposed by Andrew.

She designed the shape of her stirrer observing the amplitude level of output fields by genetic algorithm.

Since her method is an optimization-based design, it did not provide us the intuition we need for practical applications.

Right one shows that stirring performance is quantified by the number of coherence cells traversed during the stirring process

But it has limitations when dealing with fine geometries of mode stirrers.

In contrast to these methods, we will propose a more efficient spectral evaluation method.

FDTD analysis by parallel division

Angle steps of stirrer=24

f0=120MHz

f_{LUF}=500MHz

1.4 m (23λ)

1.8 m (30 λ)

2 m (33 λ)

Computation time=0.5 hr

Computation nodes= 48 (4x4x3)

6
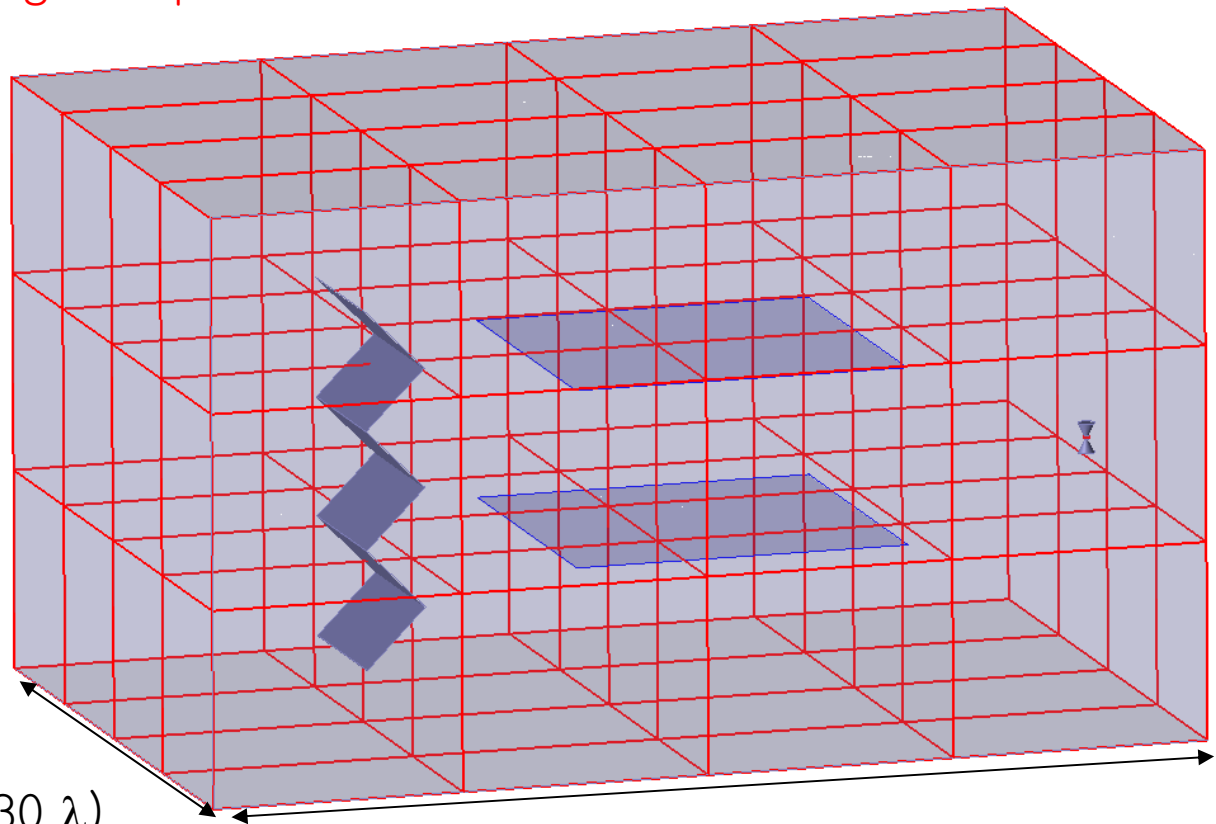
FDTD analysis by parallel division (Comments)

We simulated the chamber by using the FDTD method.

Parallel processing was used to solve this large problem efficiently.

The computational domain was divided into 4 sections along the x- and y-axis, and 3 sections along the z-axis.

We solved this problem using 48 nodes of computation cluster.

The minimum cell size was 5 mm.

Frequency range of interest was 0.5 to 5.0 GHz.

E$_z$ Field on Observation Plane (@S0:75x75cm^2) at 0.5 GHz
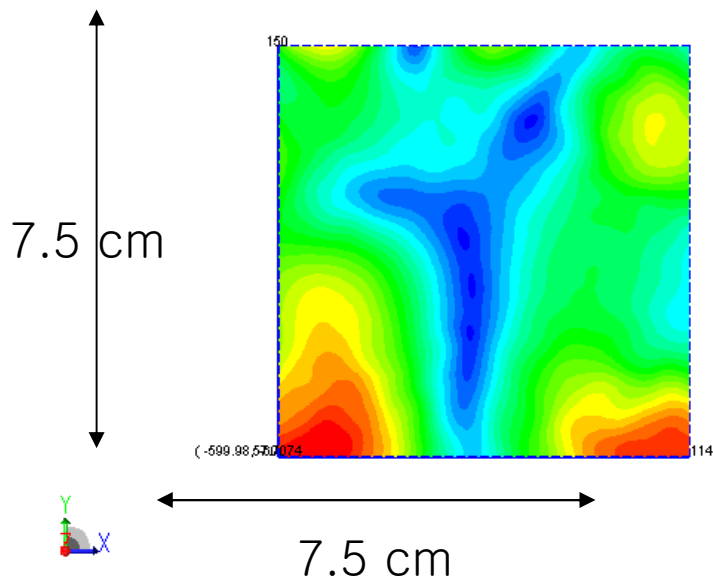
7.5 cm

7.5 cm

(a) Stirrer angle = 0°

(b) Stirrer angle = 15°

E_z Field on Observation Plane (@S0:75x75cm^2) at 0.5 GHz (Comments)

The mode stirrer in the FDTD calculation was incrementally rotated in steps of 15°.

We had 24 different angular steps.

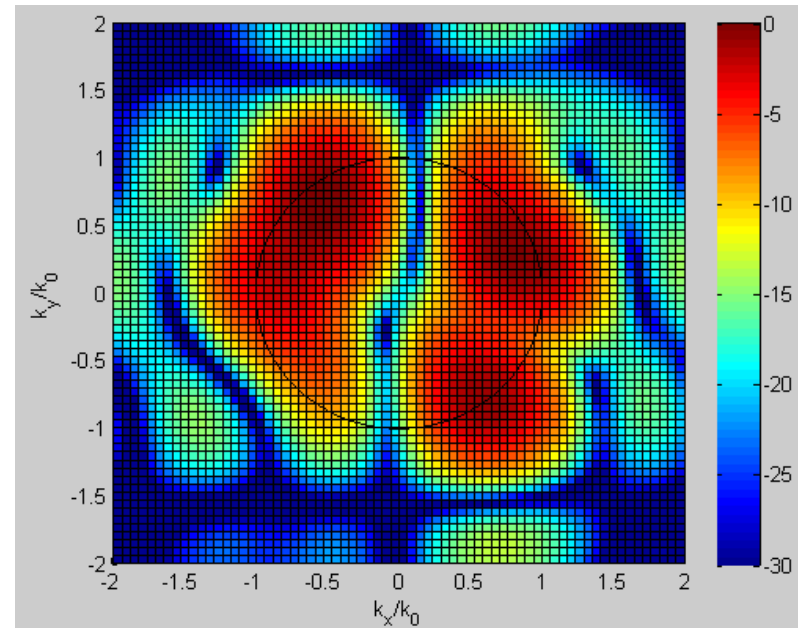Observed Ez fields at 0° and 15° are displayed here for the frequency of 0.5 GHz.

We can observe that there are large difference for these two angles.

This verifies the effectiveness of the stirrer, even for the relatively low frequencies of 0.5 MHz.

E$_z$ in Spectral Domain on Observation Plane (S0:75x75cm^2) at 0.5 GHz
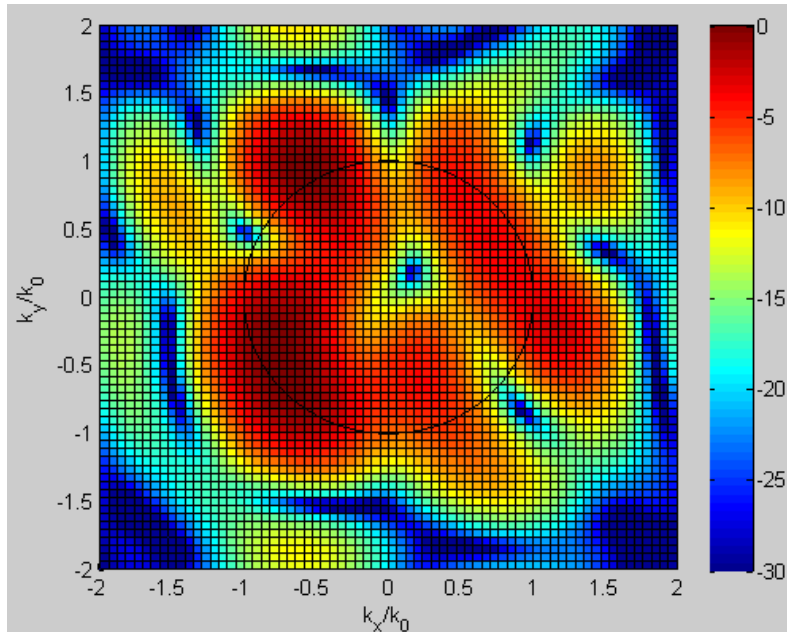
(a) Stirrer angle = 0°

(b) Stirrer angle = 15°

The propagation behaviors of Ez change over a rotating mode stirrer. The mode behaviors in RC can be found by the spectral contents

E_z in Spectral Domain on Observation Plane (S0:75x75cm^2) at 0.5 GHz (Comments)

Spectral distributions can be found by converting the observation data in the previous slide via Fourier transformation.

Magnitudes of these spectral values are indicated by the color bar in the figures.

Red color shows strong fields and blue indicates weak values.

X-axis is wavenumber kx normalized by k0 and Y-axis is wavenumber ky normalized by k0.

A unit circle is included as a boundary indicator of mode propagation in the chamber.

We can observe the directional dependence of the wave propagation at each angle.

The perturbation effect introduced by the rotating stirrer can be observed by comparing two clearly different spectral data corresponding to the two angles.
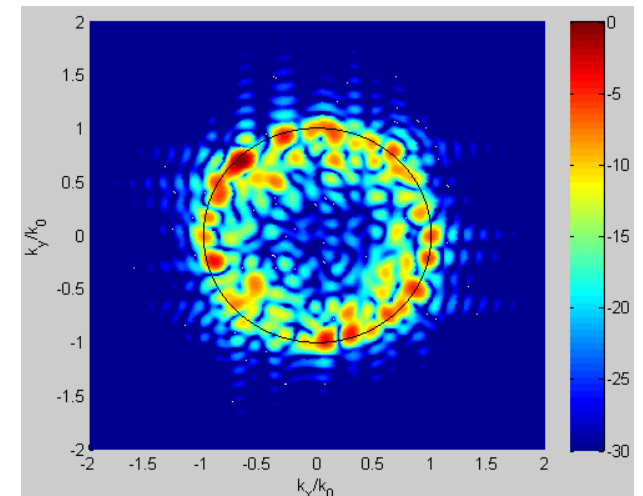
Electric Fields in Spectral Domain on Observation Plane (S0)
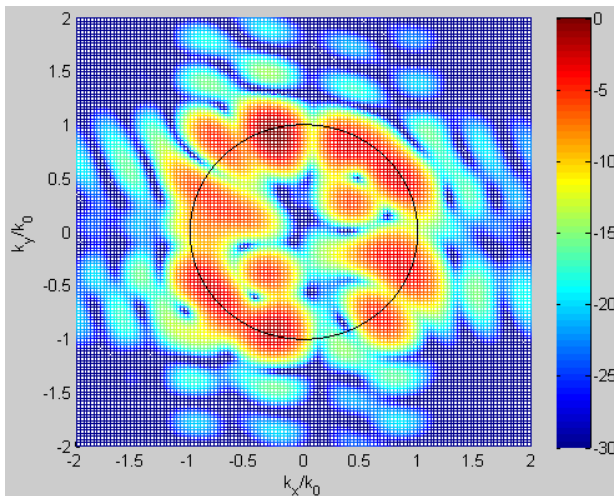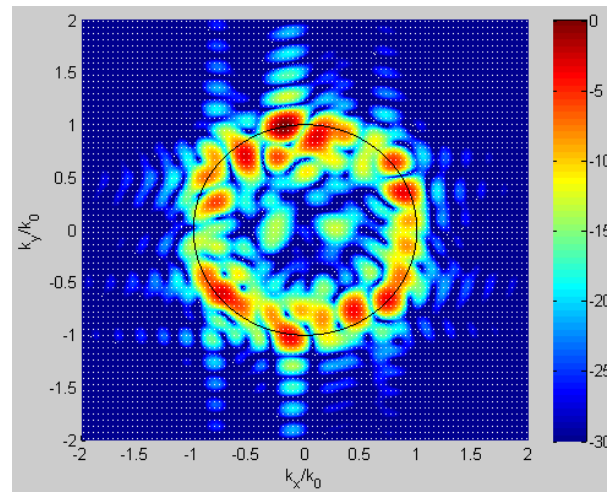
(a) 1 GHz   (b) 2 GHz   (c) 3 GHz

The spectral behaviors of Ez are shown for 1.0, 2.0 and 3.0 GHz.

Electric Fields in Spectral Domain on Observation Plane (S0) (Comments)

The spectral Ez field at 1.0, 2.0, and 3.0 GHz are displayed in this figure.

The higher the observation frequencies, the more the number of propagation modes.

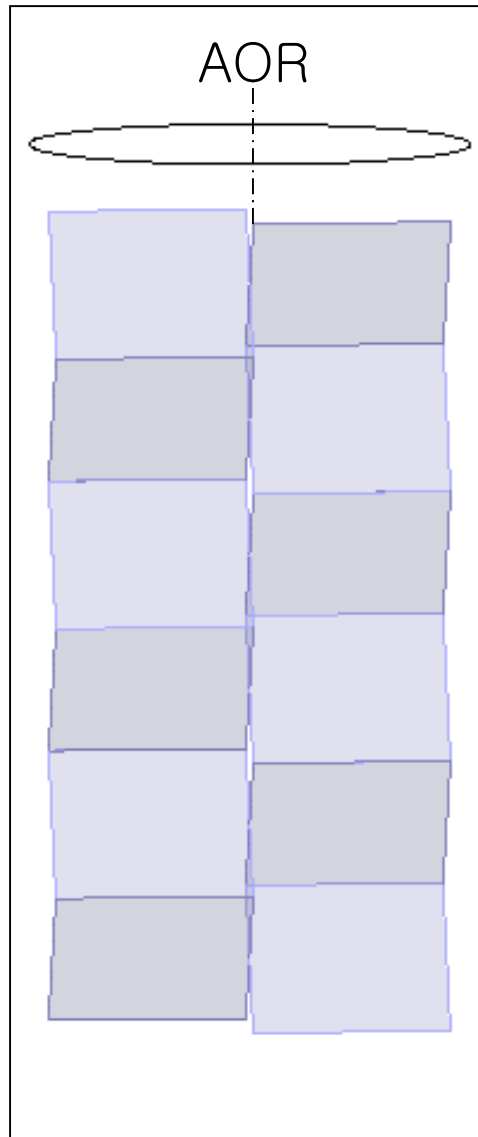Zero values near the origins indicate non-propagation at low frequencies.

We can see some banded rings of the guided mode at the excitation frequency in the chamber.

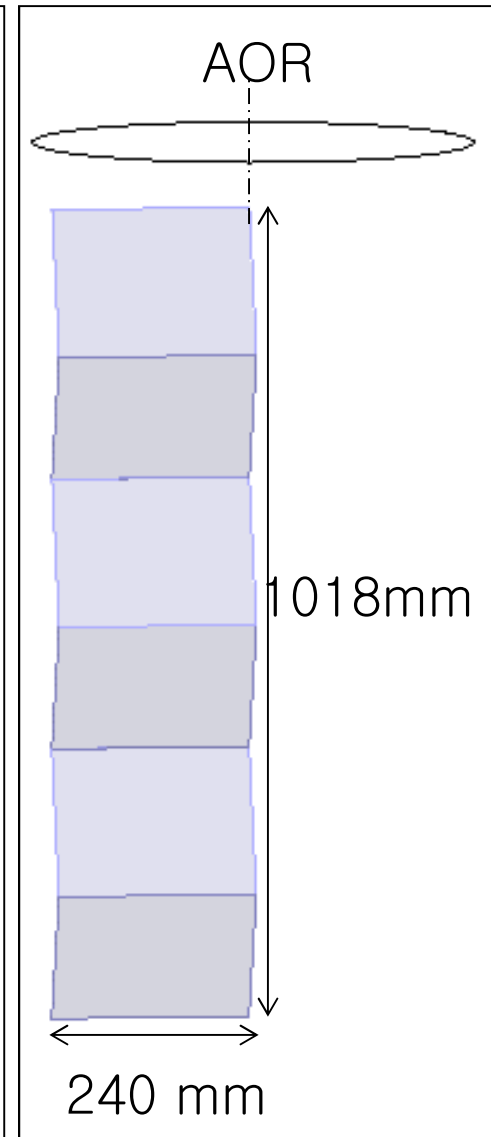# Three different stirrers' configurations

Stirrer-1 Stirrer-2 Stirrer-3

AOR   AOR   AOR

480 mm   240 mm

1018mm
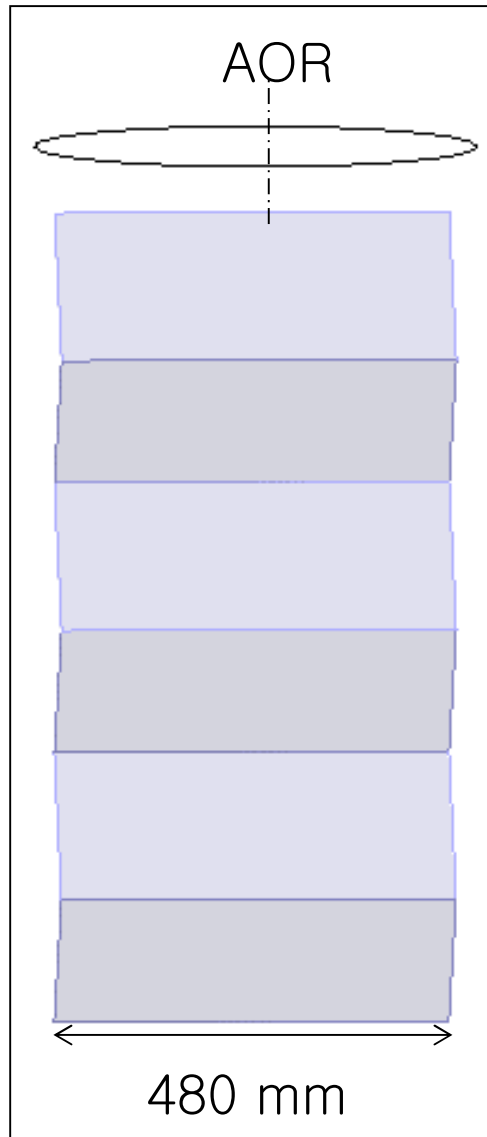
Three types of mode stirrers (Comments)

Three different designs of mode stirrer are investigated in order to verify our method.

The first stirrer is a simple type and the axis of rotation is its center.
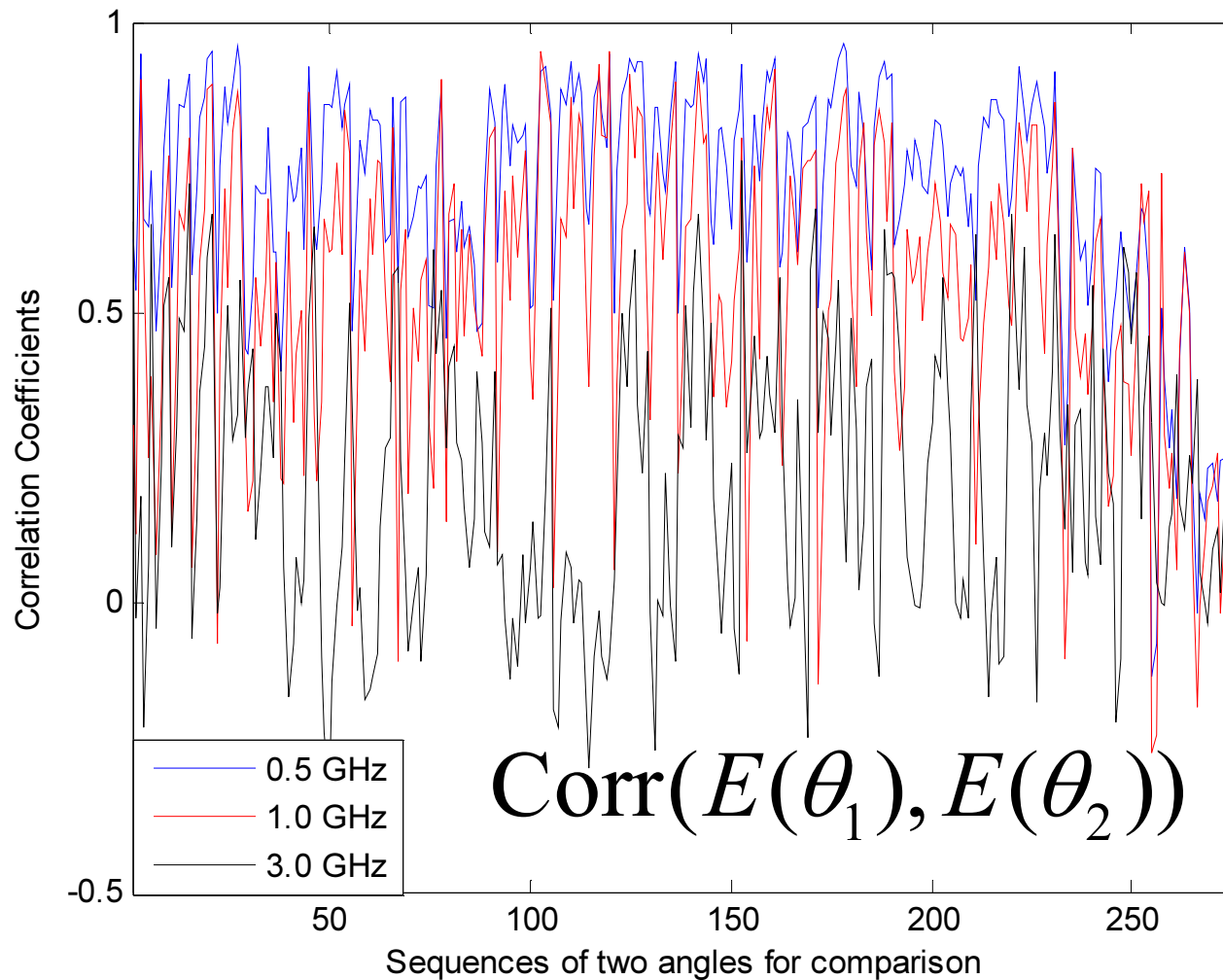
The second stirrer is obtained by converting the right half section of the stirrer-1.

Note that it is symmetric during its rotation process.

The third stirrer is found by removing the right half section of the stirrer-1.

For consistent comparison, all vertical shapes remain the same.

Correlation Coefficients between
all possible two angles of a mode stirrer−1

$\mathrm{Corr}(E(\theta_1), E(\theta_2))$

Legend: 0.5 GHz, 1.0 GHz, 3.0 GHz

Correlation Coefficients

Sequences of two angles for comparison

10

Correlation Coefficients between
all possible two angles of a mode stirrer-1
(Comments)

This plot shows the correlation coefficients of stirrer-1.

We calculate the correlation coefficient between two spectral field data at theta1 and theta2.

X-axis shows the number of angle combinations between arbitrary two angles.

We have 276 samples for 24 different angle steps.

Y-axis is correlation coefficient.

The correlation coefficient of zero represents a good result.

Blue color shows the results at 0.5 GHz.

Red and black lines show those at 1.0 and 3.0 GHz, respectively.

3 GHz has the low correlation coefficients.

It implys the independence of field values generated by the rotating mode stirrer at the higher frequency

1 GHz is next and 0.5 has the high correlation coefficients.

Statistical distributions
of correlation factors (stirrer-1)
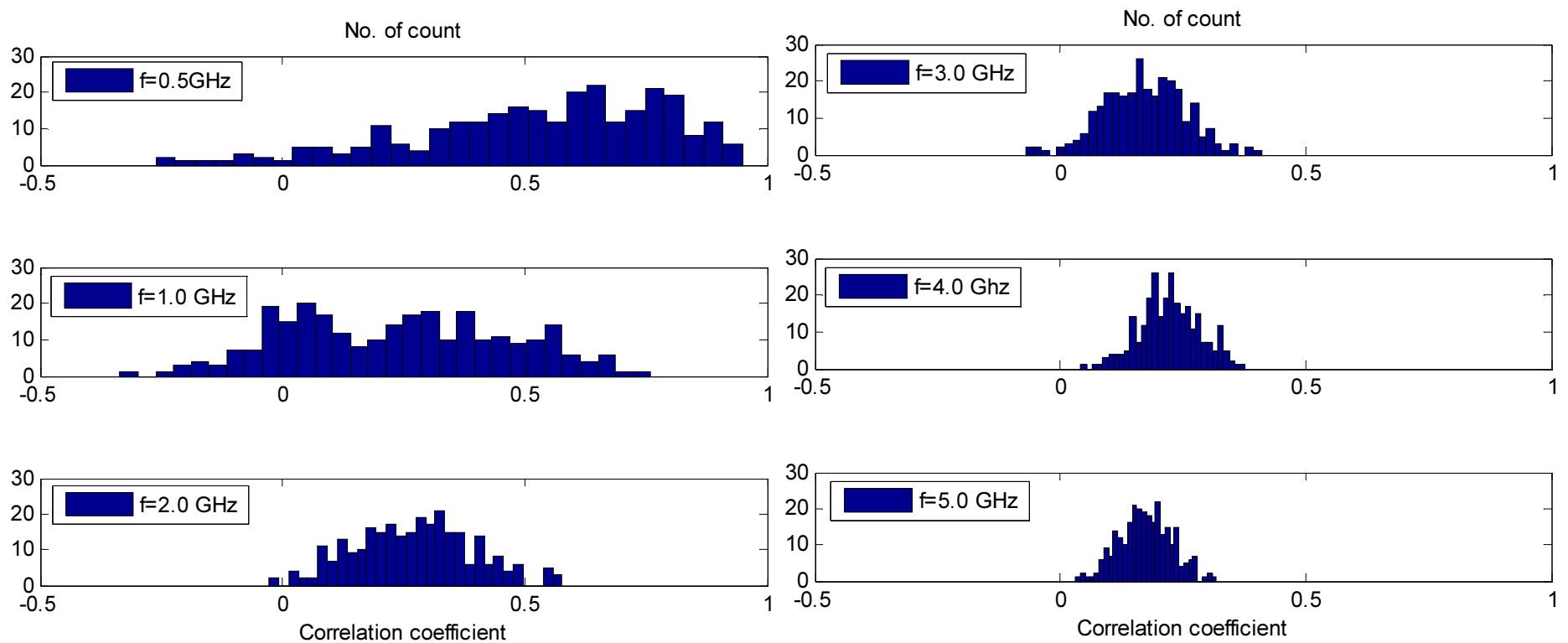
Statistical distributions
of correlation factors (stirrer-1)
(Comments)

These plots show the statistical distribution of all correlation coefficients of stirrer-1.

Results shown are for six frequencies of 0.5, 1.0, 2.0, 3.0, 4.0 and 5.0 GHz.

X-axis is correlation coefficient. Y-axis is the sample number.

Note that low frequencies are relatively spread out and high frequencies are relatively compact.

The standard deviations of the correlation coefficients at the lower frequencies are all higher.

We have a small number of excitation modes at the low frequency.

Hence, have the small changes of field values.

On the other hand, at higher frequencies, there are large changes over the rotating stirrer, owing to the increase of guided modes.

Low correlation coefficients at the higher frequencies indicate higher stirring effects.

Statistical distributions
of correlation factors for stirrer−2
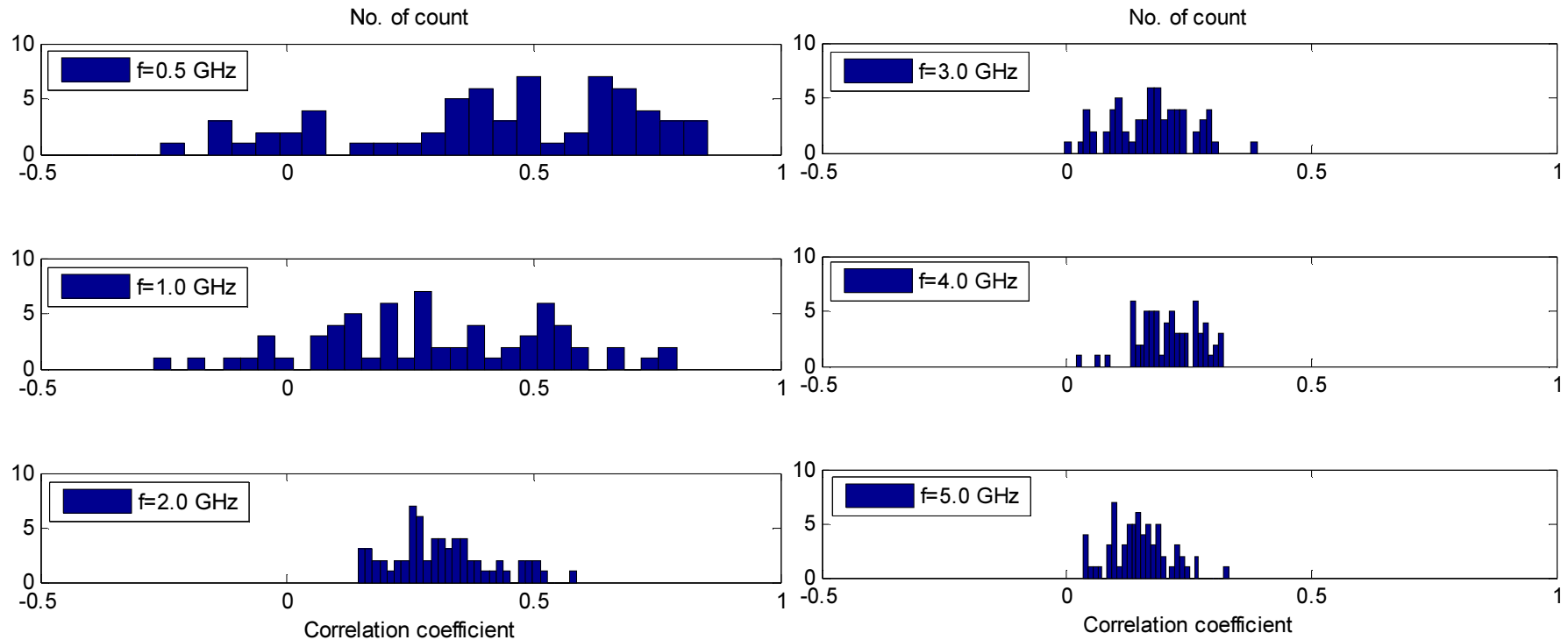
Only half the rotating states between 0° and 180° are effective due to the symmetric rotation trajectory of the stirrer.

Statistical distributions
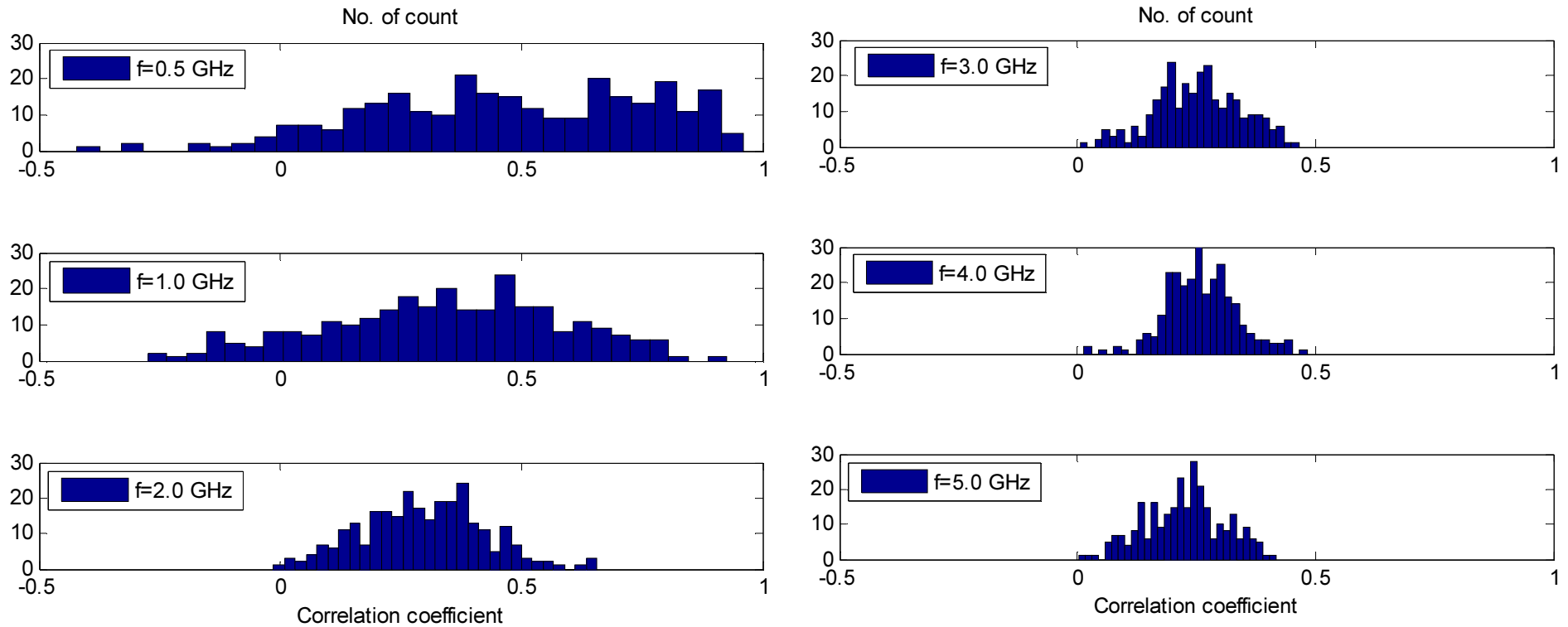# of correlation factors for stirrer-2
(Comments)

This plot shows the statistical distribution of stirrer-2.

Only half the rotating states between 0° and 180° are effective for this statistical analysis, because this stirrer is the symmetric trajectory of rotation.

We can see the small number of independent samples in the figures.

The sample number is 66, as compared to 276 for stirrer-1.

# Statistical distributions of correlation factors for stirrer−3

Statistical distributions of correlation factors for stirrer-3 (Comments)

Statistical distributions of stirrer-3 are shown for six frequencies.

Statistical variations of stirrer-3 are very similar to those of stirrer-1 for all frequencies.

Mean and standard deviation of correlation factors for three stirrers

Mean of correlation coefficients

Standard deviation of correlation coefficients

Freq. in GHz

14
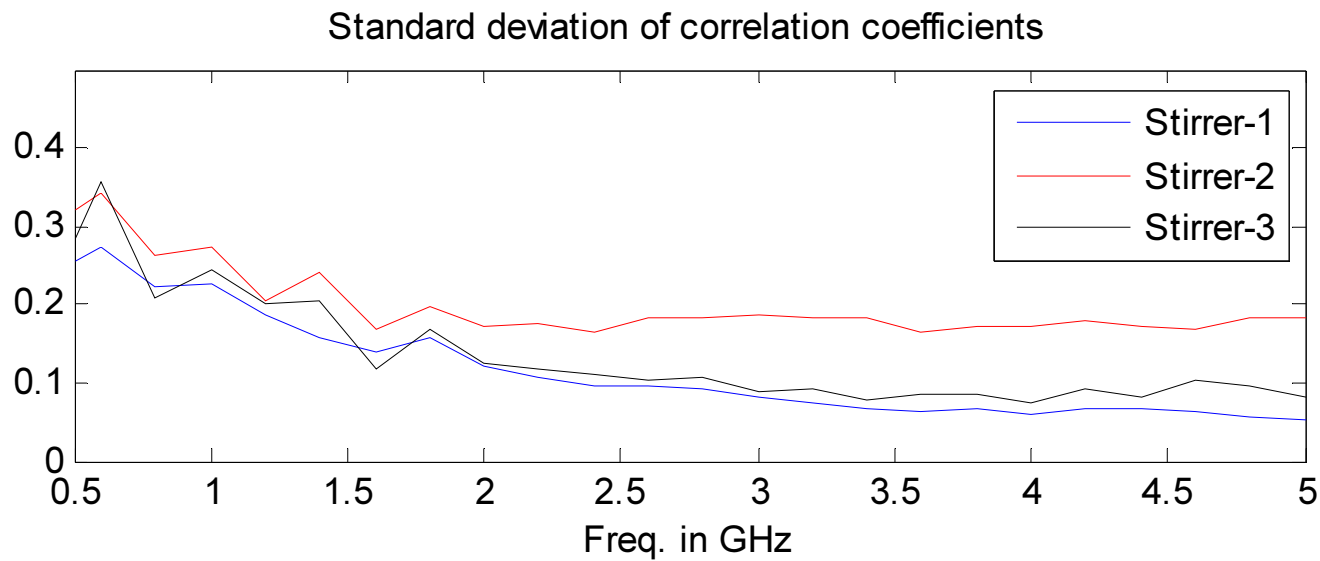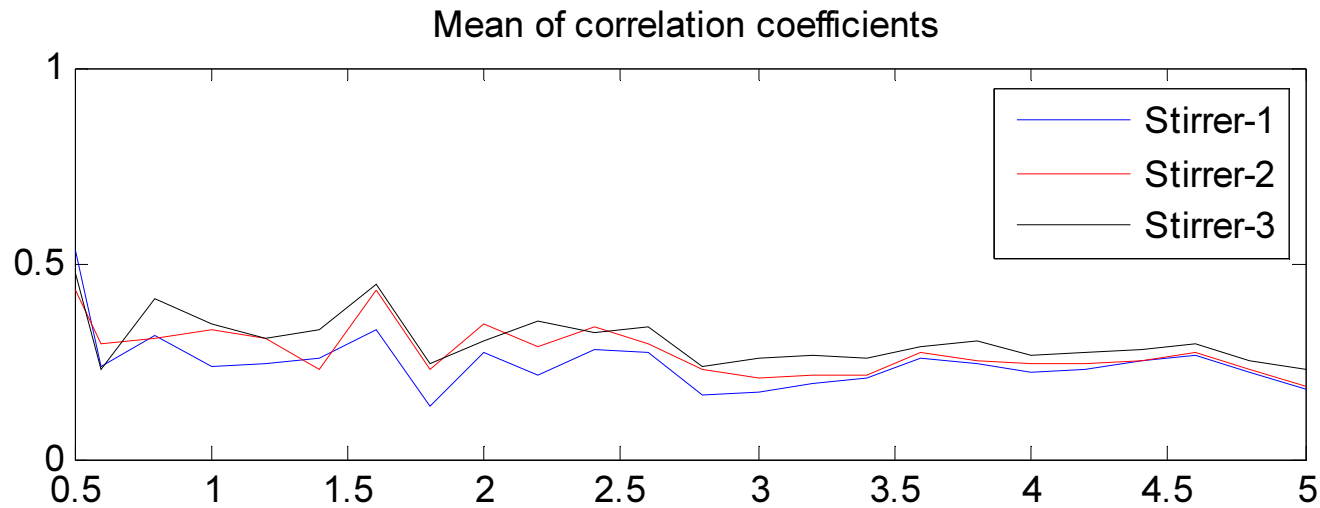
Mean and standard deviation of correlation factors for three stirrers (Comments)

The plots show the mean and standard deviation characteristics of correlation coefficients for three types of stirrers.

X-axis is the frequency band of 0.5 to 5 GHz.

Y-axis shows the mean and standard deviation of correlation coefficients.

We observe a clear difference in the characteristics of the three stirrers.

Blue color show the results of stirrer-1.

Red and black colors shows those of stirrer-2 and -3.

The averaged correlation coefficient of the stirrer-1 is the lowest among them.

Stirrer-2 is the next and stirrer-3 is inferior.

But from the lower plot, standard deviations of stirrer-1 and -3 is lower.

Stirrer-2 is high due to its symmetric rotation shape by stirrer-2.

From our spectral method, the higher the operating frequency, the better the stirring performance, as expected.

Investigation of field uniformity by statistical analysis

$$Std\_dB=20*log(1+std(E)/mean(E))$$

15
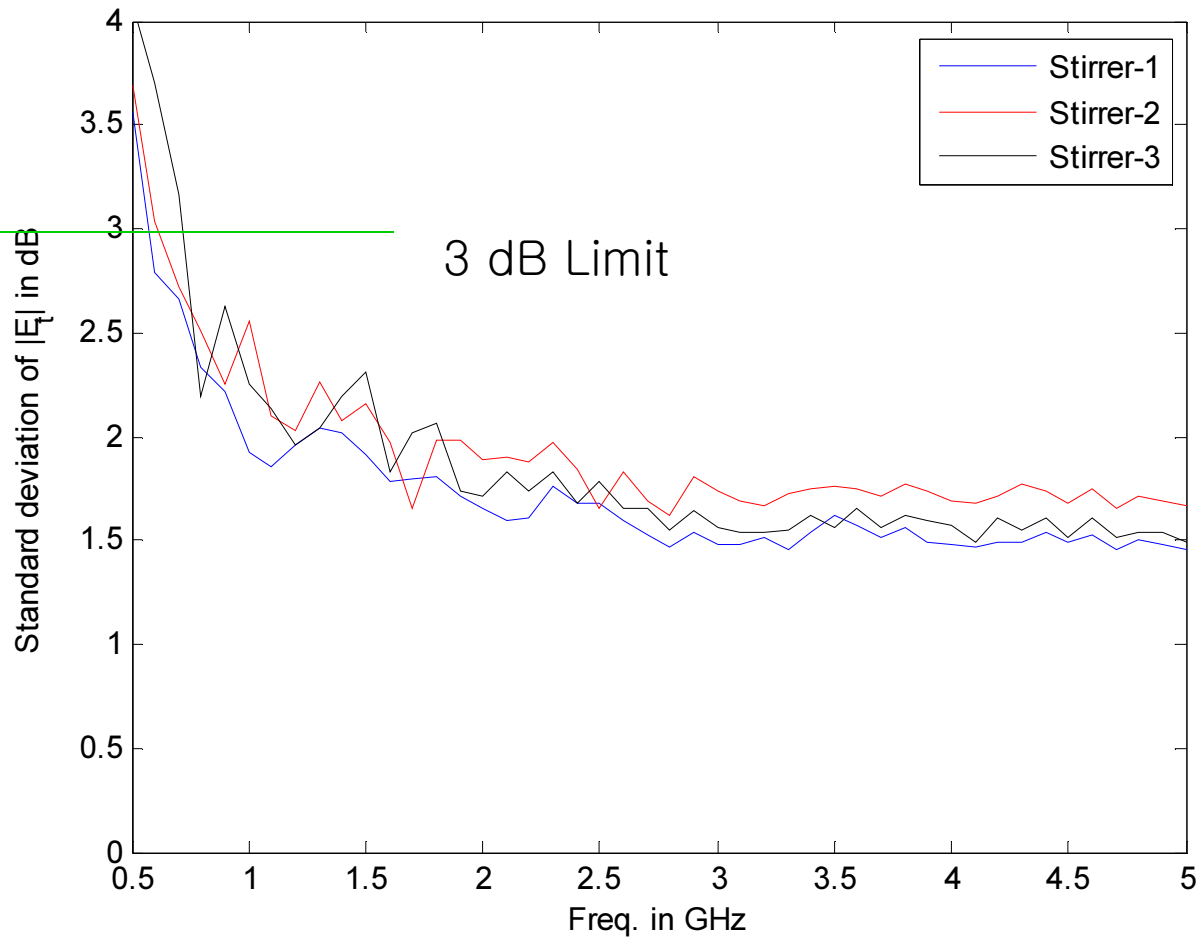
Investigation of field uniformity by statistical analysis (Comments)

We can compare our result with the statistical results.

The plots show the standard deviations obtained by using the statistical analysis.

While there are large values at lower frequencies, uniformity is achieved for frequencies above 1 GHz.

We can see stirrer-1's performance is the best and stirrer-3 is the second best.

Poor performance of stirrer-2 is to be expected for reasons given above in slide No.12.

There is good agreement with our spectral method.

Conclusions

- Stirring effects in the RC were investigated in terms of correlation coefficients in spectral domain.

- Three different stirrers were employed in the RC and the results obtained were compared with each other.

- Good agreement was found between the statistical results and spectral evaluation.

Conclusions (Comments)

We summarize this talk with a few concluding remarks:

Stirring effect of the RC can be evaluated by examining the correlation coefficients of the field data in spectral domain.

To validate our method, three different stirrers were employed and the corresponding results were compared.

The presented method can be a good estimator of the performance during the process of designing the stirrer.

The method can be applied to any shape or type of RC.